Global Measurement of Non-Photosynthetic Vegetation

Response to the Decadal Survey for Earth Science and Applications from Space RFI2

Authors

Philip E. Dennison, University of Utah
Dar A. Roberts, University of California Santa Barbara
Jeffrey Q. Chambers, University of California Berkeley
Craig S. T. Daughtry, USDA Agricultural Research Service
Juan Pablo Guerschman, CSIRO Land and Water, Australia
Raymond F. Kokaly, USGS, Denver, Colorado
Gregory S. Okin, University of California Los Angeles
Peter F. Scarth, University of Queensland, Australia
Pamela L. Nagler, USGS Southwest Biological Science Center
Christopher J. Jarchow, USGS Southwest Biological Science Center

Summary

Terrestrial vegetation is dynamic, expressing seasonal, annual, and long-term changes in response to climate and disturbance. Phenology and disturbance (e.g. drought, wildfire, and insect outbreak) can cause a transition from photosynthesizing "green" vegetation to non-photosynthetic vegetation (NPV). NPV includes dead and senescent vegetation, plant litter, and non-photosynthesizing branch and stem tissues. NPV cover, measured as the fractional abundance of NPV by area, is a critical and poorly quantified constituent of natural and agricultural ecosystems. Measurements of NPV cover can quantify vegetation response to seasonal and long-term drought, mortality caused by disturbance events, wildfire impacts, crop residue cover and susceptibility to erosion, and forage conditions. With increasing temperature and increasing precipitation variability, NPV dynamics will be an essential metric of climate change impacts on vegetation. To advance Earth science and applications under Theme III, this paper proposes a measurement objective to "map seasonal NPV cover for all vegetated ecosystems globally at a spatial resolution required for quantifying stand/patch scale variation (≤ 30 m)."

NPV cover can be measured using lignin and cellulose absorption features in the shortwave infrared (SWIR), over a range of 2000-2450 nm. Measurements currently used for quantifying terrestrial ecosystem processes dominantly rely on remote sensing of photosynthesizing vegetation (e.g. NDVI and related indices) and cannot fully resolve lignocellulose absorption features, making it difficult to separate NPV cover from background soil cover. Current imaging spectrometer technology is capable of resolving lignocellulose absorption features required for mapping NPV cover. Our measurement objective can be achieved at 30 m spatial resolution using an imaging spectrometer with a spectral resolution ≤ 15 nm, a 185 km swath, and a 16-day revisit period. NASA-guided engineering studies have confirmed that a mission with these characteristics can be affordably implemented, a prototype instrument has been developed, and multiple airborne imaging spectrometer campaigns have tested the data processing algorithms needed for a global NPV mapping mission.

1. Science and Application Target: Non-Photosynthetic Vegetation (NPV)

Measurements used for quantifying terrestrial ecosystem processes, mapping land cover change, and modeling global change are almost exclusively based on remote sensing of photosynthesizing "green" vegetation. Current measurements, including multiple Essential Climate Variables (ECV), do not capture NPV, representing plant litter, senescing foliage, branches, and stems (Roberts et al, 1993; Nagler et al., 2000). Plant biochemical constituents comprising NPV include lignin and cellulose, which are the most abundant molecules produced by the photosynthetic activity of terrestrial vegetation. Collectively and individually, NPV components play a crucial role in terrestrial ecosystems, directly affecting carbon and nutrient cycling, erosion, and wildfire danger. Large, globally relevant fluxes of carbon from live to dead pools are strongly correlated with shifts in NPV cover. Measures of NPV are required to fully address biochemical and functional attributes of terrestrial ecosystems captured in Earth Science Theme III: Marine and Terrestrial Ecosystems and Natural Resource Management. Using lignin and cellulose spectral features in the shortwave infrared (SWIR; 1.4-2.5 µm), NPV cover measured as fractional abundance of NPV by area is quantifiable using current technology (Kokaly et al., 2009; Lee et al., 2015; Singh et al., 2015).

Terrestrial vegetation is dynamic, and varies on seasonal, annual, and decadal scales. Temporal variations in climate (temperature, precipitation, and their seasonality) and disturbance affect the relative cover of photosynthetic vegetation (PV) and NPV in terrestrial ecosystems. For example, grasslands senesce during periods of seasonal drought, mountain pine beetle outbreaks result in widespread mortality of pine forests, and long-term drought can result in increased NPV in vegetation ranging from agricultural crops to native shrubs and trees. Commonly, changes in NPV cover are inferred using vegetation indices sensitive to greenness (e.g. NDVI and related indices). However, spectral measures that do not resolve lignocellulose absorption in the SWIR are unable to separate NPV cover from the background substrate (soil) (Figures 1-2). NPV cover is an important source of error in relationships between vegetation indices and biophysical variables (Figure 3) (Van Leeuwen & Huete, 1996; Nagler et al., 2000), and a mixture of PV and soil cover has very different implications for productivity and carbon storage than a mixture of PV and NPV cover (Asner et al., 2003).

Changes in NPV cover are often closely related to drought. Seasonal drought can be expressed as a change in the ratio of live to senesced foliage (Roberts et al. 1997; 2006; Elmore et al., 2000; Okin, 2010). Increases in NPV cover over longer time scales can indicate differences in species susceptibility to water stress (Figure 4). During the extreme drought in California, remote sensing measurements have shown strong increases in NPV cover for more shallowly rooted species, dependent on topography (Coates et al., 2015), as well as decreased canopy moisture content (Asner et al., 2016). Plant pathogens or any form of disturbance that leads to leaf shedding or senescence can be quantified by examining changes in NPV cover. Small scale wind disturbances and associated tree mortality in the Amazon can be mapped at subpixel scales as an increase in fractional NPV cover, and accurate estimates of these disturbance fluxes are essential for quantifying regional carbon balance (Negrón-Juárez et al., 2011; Chambers et al., 2013). Satellite-derived NPV metrics were also employed to quantify regional tree mortality and canopy damage following the landfall of Hurricane Katrina in Gulf Coast forests (Figure 5; Chambers et al., 2007).

NPV is an important component of many managed ecosystems, including agricultural and pasture systems. In agricultural systems, plant residues represent an important source of future organic carbon for soils and are the first line of defense against the erosive forces of wind and water (e.g., McGregor and Greer, 1982; Karlen et al., 1994; Nagler et al., 2000; Lal et al., 2007). After harvest, NPV (crop residue) often completely covers the soil surface, but when the soil is tilled or NPV is harvested for feed or biofuel, NPV cover decreases (Daughtry et al., 2006; Serbin et al., 2013). Quantification of fractional NPV cover on the soil surface after crops are planted is crucial for monitoring soil tillage intensity and assessing the extent of conservation practices in agricultural landscapes (Daughtry et al., 2012). Thus, managing NPV cover on soil surfaces is often a crucial component for sustainable agronomic production (Delgado, 2010).

As a component of total ground cover, NPV is critical for effective monitoring and modelling of catchment wide erosion processes and for the assessment of land management changes on water quality outcomes (Karfs et al. 2009; Star et al., 2013; Beutel et al., 2014). In pastoral systems and pastures, NPV provides valuable ecosystem services, often representing the dominant form of carbon remaining after grazing (e.g., Herrick et al., 2005; Scarth et al., 2010; Meyer & Okin, 2015). The ratio of live to senesced grass cover is an important measure of the degree of degradation in pastures, with degraded pastures in the Amazon often showing a significant increase in the ratio of senesced to live grass, as cattle preferentially consume green foliage and leave NPV behind (Numata et al., 2007; Davidson et al., 2008). In pasture communities that rely on episodic rainfall events, such as in arid and savanna ecosystems, estimates of NPV cover are the only way to objectively separate grazing effects on ground cover from those due to interannual variation in rainfall (Bastin et al., 2012).

Wildfire is a globally important ecosystem disturbance that has critical impacts on carbon and particulate emissions. As vegetation senesces, canopy water content decreases and the expression of lignocellulose absorption increases (Figure 6). Senescence and the “curing” of fuels leads to increased fire danger. Fractional NPV cover is correlated with fuel moisture content, and can be used to measure seasonal changes in fire danger (Roberts et al., 2006). Changes in NPV cover can indicate build-up of fine fuel biomass over time (Elmore et al., 2005), and NPV cover can also be used to map fuel types and disturbance (Jia et al., 2006). Post-fire NPV is correlated with the presence of charred organic material (Lewis et al., 2007), can be used to map burn severity (Van Wagtendonk et al., 2004; Veraverbeke & Hook, 2013; Veraverbeke et al., 2014), and reveal areas of vegetation killed (but not consumed by) wildfire (Kokaly et al., 2007; Lewis et al., 2011).

Even though NPV can represent the dominant form of aboveground biomass in many ecosystems, is an important indicator of disturbance, and plays a key role in biogeochemical cycles, there is currently limited capability for global and seasonal mapping of NPV cover. To address the need for improved understanding of the role of NPV cover in terrestrial ecosystems, we propose the following measurement objective:

Map seasonal non-photosynthetic vegetation cover for all vegetated ecosystems globally at a spatial resolution required for quantifying stand/patch scale variation (≤ 30 m)

2. Utility of NPV Cover for Earth Science and Applications

Global, seasonal measurement of NPV cover will facilitate critical advances in science and applications within Earth Science Theme III. Measurement of NPV cover will help quantify how vegetation phenology responds to short-term and long-term climatic variability (Roberts et al., 1997; Coates et al., 2015). Separation of NPV from soil is essential for understanding how vegetation cover, forage, and fuels vary from year to year in response to climate and human impacts (e.g. Pasto et al., 1957; Asner & Heidebrecht, 2005; Littell et al., 2009; Bastin et al., 2012). A key benefit of NPV cover measurements will be quantification of the impacts of disturbance on ecosystems, including drought, wildfire, extreme wind events, and insect outbreaks (Asner & Heidebrecht, 2005; Chambers et al., 2007; Kokaly et al., 2007; Coates et al., 2015). Changes in NPV cover can provide both the magnitude of disturbance and be used to model the carbon implications of disturbance (Chambers et al., 2007). Seasonal NPV cover and its seasonal and interannual variability will have utility for mapping vegetation types with differing phenology and climatic response, such as invasive grass species (Bradley & Mustard, 2006). Separation of NPV from soil may also assist in quantifying soil organic carbon in semi-arid or arid ecosystems (Asner et al., 2003). For agricultural lands, soil tillage intensity is characterized by the fraction of the soil surface covered by crop residue (NPV) after planting. Currently, no program exists for objectively and uniformly quantifying agricultural NPV cover at appropriate spatial scales over large areas. Mapping crop residue cover will provide improved understanding of the spatial and temporal variability of carbon fluxes and soil carbon loss due to erosion across agricultural landscapes (Daughtry et al., 2012; Star et al., 2013; Beutel et al., 2014). NPV cover products will be used to refine, improve, and extend applications developed for monitoring forage conditions, like VegMachine (Figure 7) (Beutel et al., 2005). NPV cover measurement will also assist the development of monitoring products derived from complementary, coarser spectral and/or spatial resolution instruments like Landsat, Sentinel-2, MODIS, and VIIRS.

3. Key Requirements

Multispectral, broadband systems such as Landsat TM/OLI and MODIS/VIIRS cannot fully resolve lignocellulose absorption, and thus the ability of these sensors to accurately map NPV cover has been found to be moderate or limited (e.g. Scarth and Phinn, 2000; Numata et al., 2008; Guerschman et al., 2009; 2015; Zheng et al., 2013; Meyer & Okin, 2015). The ability to discriminate NPV from soils is entirely dependent upon 1) sensor bands and noise, 2) the ability to adequately remove atmospheric and BRDF effects, and 3) whether background substrates are broadly distinct from senesced vegetation, which is true in many, but not all systems (Okin et al., 2001; 2004; Nagler et al., 2003; Daughtry et al., 2005; Okin & Gu, 2015). Furthermore, even in cases where NPV cover can be mapped, continuous spectra provide higher levels of accuracy (Okin et al., 2004; Numata et al., 2008; Serbin et al., 2009a) and improve atmospheric correction which also helps discriminate NPV from soil (Okin & Gu, 2015). Thus, SWIR spectroscopy is required to definitively discriminate NPV from abiotic substrates (e.g. soils, rock or man-made materials) in the presence of significant natural variation, and is essential for measuring low percentages of NPV cover (Elvidge, 1990; Roberts et al., 1993; Daughtry, 2001; Okin et al., 2001; Nagler et al., 2003; Kokaly et al. 2009).

Global mapping of fractional NPV cover will require continuous spectra over a minimum spectral range of 2000 to 2450 nm, capturing lignocellulose and mineral absorption features that allow separation of NPV from soil (e.g. Asner & Heidebrecht, 2002; Serbin et al., 2009b; Kokaly et al., 2013), plus a portion of the near-infrared (NIR) spectrum covering one of the water vapor absorption features (around 940 or 1140 nm) for atmospheric correction (Gao & Goetz, 1990; Gao et al., 2009). Expanding the spectral range to 400-2500 nm would enable improved discrimination of NPV from PV by capturing chlorophyll absorption in the visible and the full range of canopy and soil liquid water absorption in the NIR and SWIR. This expanded spectral range will also allow greater accuracy in atmospheric correction, by covering additional atmospheric water vapor absorptions in the NIR. It is important to achieve accurate atmospheric correction because residual, uncorrected atmospheric water vapor will have strong impacts at the edges of lignocellulose absorption features in the 2000 to 2450 nm range. Spectral resolution and full-width half-maximum must be ≤ 15 nm to have full discrimination of NPV from other cover types (Figure 8). Measures used to quantify lignocellulose absorption and NPV cover, including spectral mixture analysis (e.g. Roberts et al., 1993; Asner & Heidebrecht, 2002), band depth analysis (e.g. Kokaly & Clark, 1999; Daughtry et al., 2004) and partial least squares regression (e.g. Serbin et al., 2014; Qi et al., 2014) will also provide higher accuracies with greater spectral sampling. Fractional NPV cover measurements will have a targeted 1σ error ≤ 5%. Additional science is needed to demonstrate that this level of accuracy is achievable globally.

Our measurement objective can be achieved at 30 m spatial resolution using an imaging spectrometer with a 185 km swath and a 16-day revisit period. The revisit requirement is ultimately driven by the need for seasonal cloud-free coverage. Ninety percent seasonal coverage of terrestrial ecosystems is desirable for NPV cover mapping. Mercury et al. (2012) found that three-month coverage of land surface and coastal areas ranged from 76% (Oct-Dec) to 86% (Jan-Mar & Apr-Jun) for a mission design with a 19-day revisit period (Figure 9). Shortening the revisit period to 16 days should exceed or come close to 90% seasonal coverage of terrestrial ecosystems, with the potential exception of the Oct-Dec period. The areas least likely to have seasonal coverage are very high latitude, tropical forests, or impacted by the Asian monsoon (Figure 9).

Radiometric requirements include capturing the full range of reflected solar radiance from zero to the maximum Lambertian reflectance for vegetated terrestrial ecosystems, high radiometric sampling (≥12 bit), and ≥90% radiometric accuracy in the SWIR. High spectral uniformity is needed for consistent fractional cover mapping, restricting geometric distortions (spatial keystone) to ≤10% and cross-track distortions (spectral smile) to ≤10%. A Level 3 fractional NPV cover product can be generated from Level 2 apparent surface reflectance. Atmospheric correction of Level 1B top-of-atmosphere radiance to Level 2 apparent surface reflectance would greatly benefit from an expanded spectral range that includes aerosol (400-700 nm), oxygen absorption (762 nm) and water vapor absorption spectral features.

4. Achieving Global NPV Measurements in the Decadal Timeframe

Global NPV measurements can be achieved affordably in the decadal timeframe, due to investments in response to global imaging spectrometer missions proposed in the 2007 NRC

Decadal Survey (NRC, 2007) and 2013 NRC sustainable land imaging report (NRC, 2013). An imaging spectrometer mission to measure NPV would build on a legacy of airborne and space instruments including AIS (Vane et al., 1984), AVIRIS (Green et al., 1998), AVIRIS-NG (Hamlin et al., 2011) and Hyperion (Pearlman et al., 2003), as well as NIMS (Carlson et al., 1992), VIMS (Brown et al., 2004), Deep Impact (Hampton et al., 2005), CRISM (Murchie et al., 2007), M3 (Green et al., 2011), and MISE, the imaging spectrometer now being developed for NASA's Europa mission.

NASA-guided engineering studies in 2014 and 2015 showed that a global terrestrial VSWIR (380 to 2510 nm) imaging spectrometer with a 185 km swath, 30 m spatial sampling and 16-day revisit with high signal-to-noise ratio and the required spectroscopic uniformity can be implemented affordably for a three year mission with mass, power, and volume compatible with a Pegasus-class launch vehicle (Mouroulis et al., 2016). A scalable prototype F/1.8 full VSWIR spectrometer (van Gorp et al., 2014) has already been developed and aligned, and qualification is being completed (Figure 10). Data rate and volume issues have been addressed by development and testing of a lossless compression algorithm for spectral measurements (Klimesh et al., 2006; Aranki et al., 2009a,b; Keymeulen et al., 2014). This algorithm is now a Consultative Committee for Space Data Systems standard (CCSDS, 2015). Algorithms for automated cloud screening (Thompson et al., 2014), calibration (Green et al., 1998), and atmospheric correction (Gao et al., 1993, 2009; Thompson et al., 2015) have been tested as part of the HyspIRI preparatory (Lee et al., 2015), NASA AVIRIS-NG India, and SIMPL Greenland campaigns. Spectral analysis algorithms have been applied to identify and map materials using airborne imaging spectrometer data collected over a large area of Afghanistan (>430,000 sq.km.) and over an extended time period (more than two months), demonstrating consistent discrimination of NPV from soil mineral components (Kokaly et al., 2013). To enhance affordability and accelerate measurement availability, there is good potential for international partnerships.

Figures

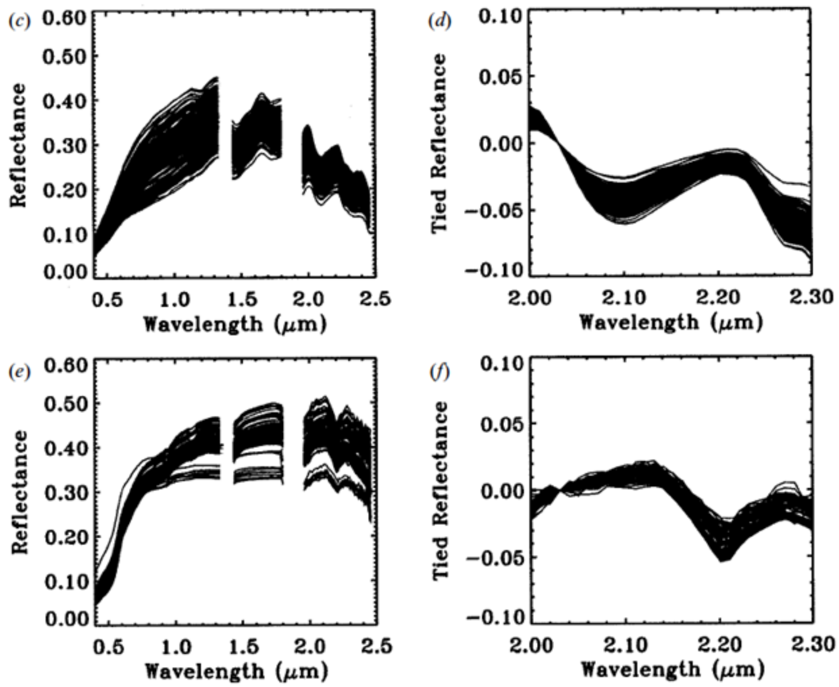

Figure 1. Spectral variability in NPV (top-left) and soils (bottom-left). Much of this spectral variability occurs in the SWIR, which can be seen when spectra are tied to a fixed wavelength at 2040 nm (panels at right). From Asner & Heidebrecht, 2002.

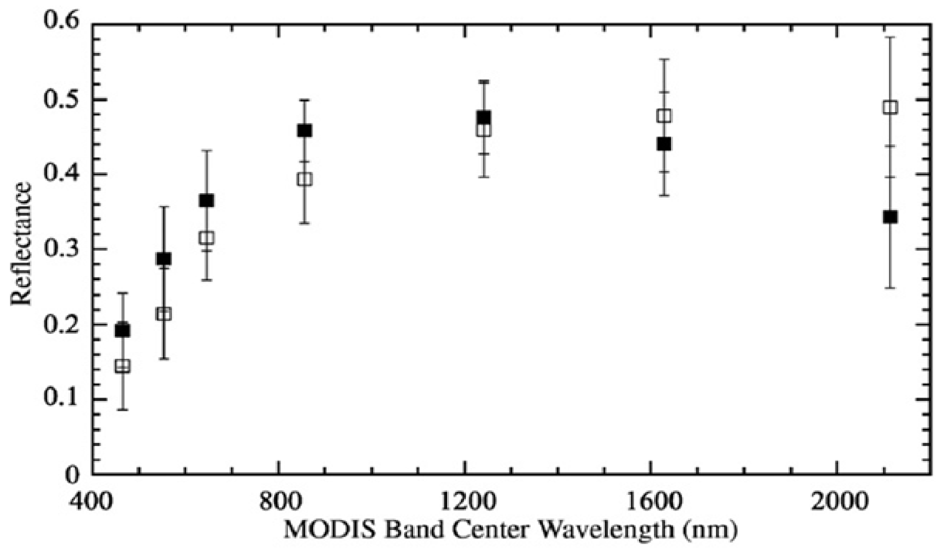

Figure 2. The spectral signatures of NPV (filled squares) and soils (open squares) are difficult to separate without a continuous spectrum capturing lignocellulose absorption in the SWIR. The example shown is for MODIS data. From Okin, 2007.

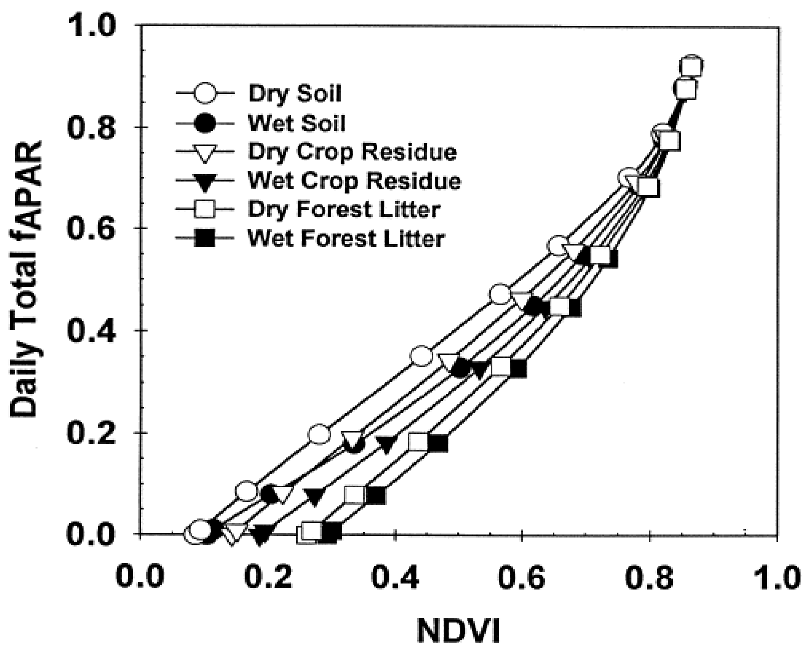

Figure 3. The relationship between NDVI and fraction of absorbed photosynthetically active radiation (fAPAR) as it varies by background substrate, including soil and two types of NPV (crop residue and litter). From Nagler et al., 2000.

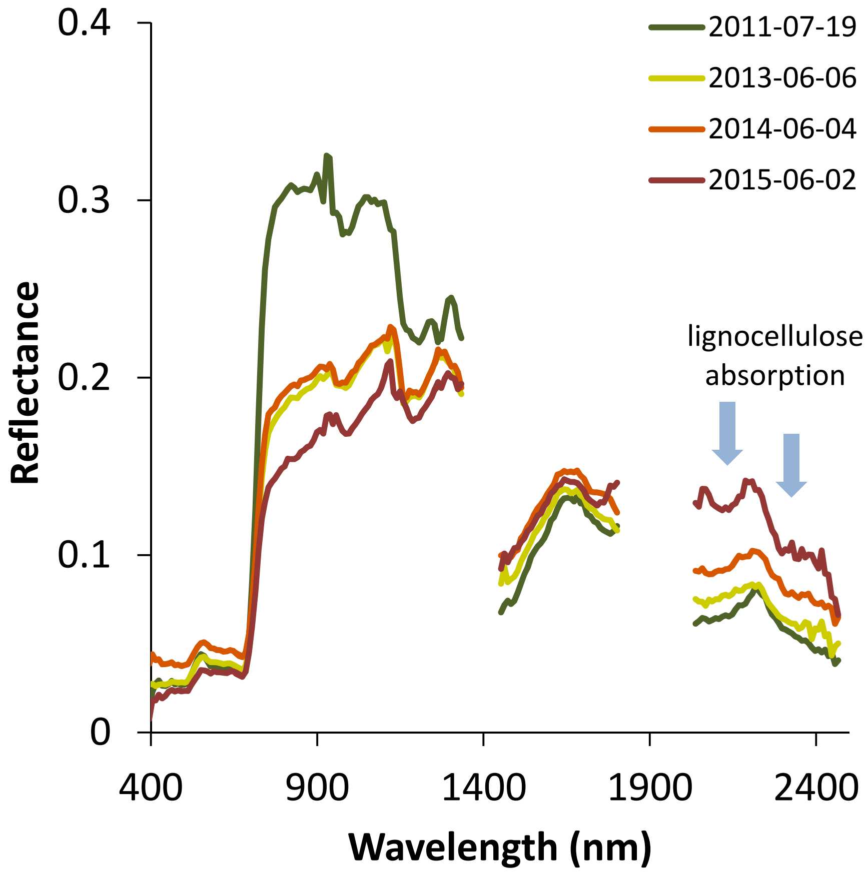

Figure 4. Changes in spectral reflectance over time in a single pixel containing *Ceanothus megacarpus.* Changes in spectra measured by AVIRIS capture canopy dieback caused by the California drought. Expression of lignocellulose absorption has increased as canopy dieback has occurred, indicating an approximate 50% increase in fractional NPV cover. Adapted from Coates et al., 2015.

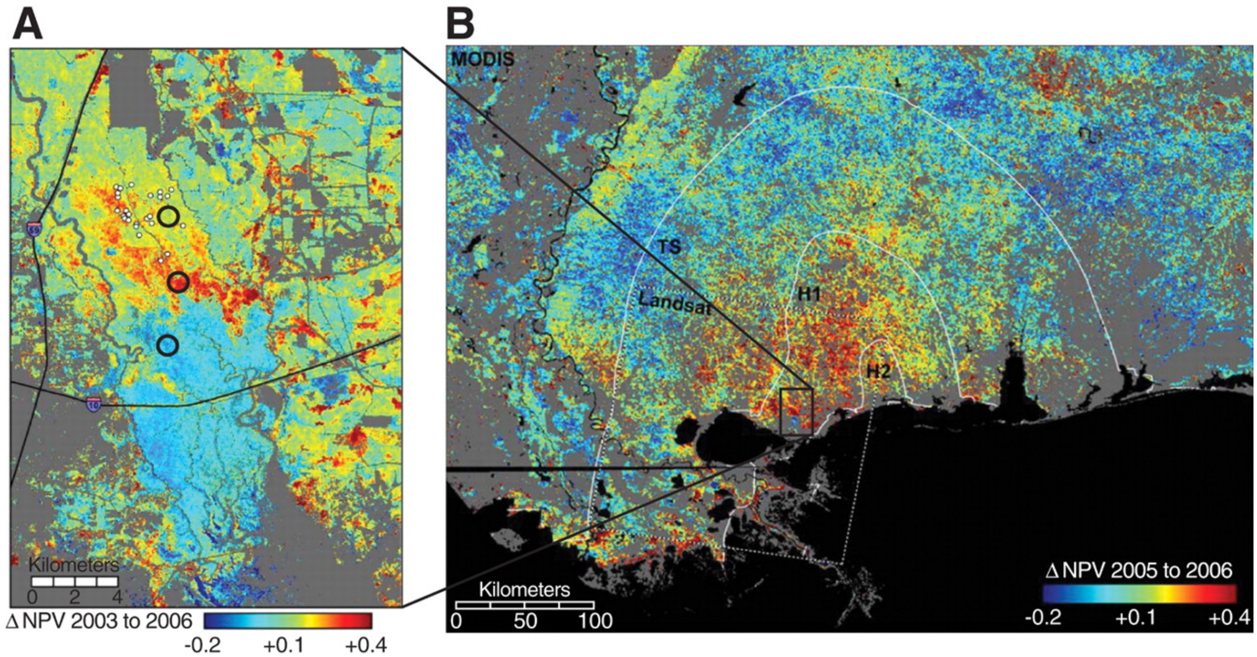

Figure 5. Change in NPV cover modeled from Landsat TM (A) and MODIS (B) data following landfall of Hurricane Katrina in 2005. White lines in (B) indicate areas experiencing hurricane (H2 & H1) and tropical storm (TS) force winds. From Chambers et al., 2007.

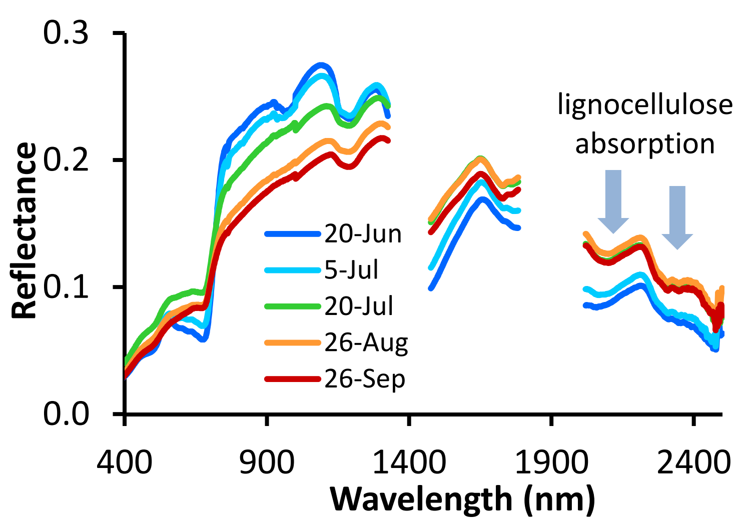

Figure 6. Seasonal changes in big sagebrush (*Artemisia tridentata*) reflectance. As sagebrush senesces through the summer and fall, NPV cover increases and fire danger increases.

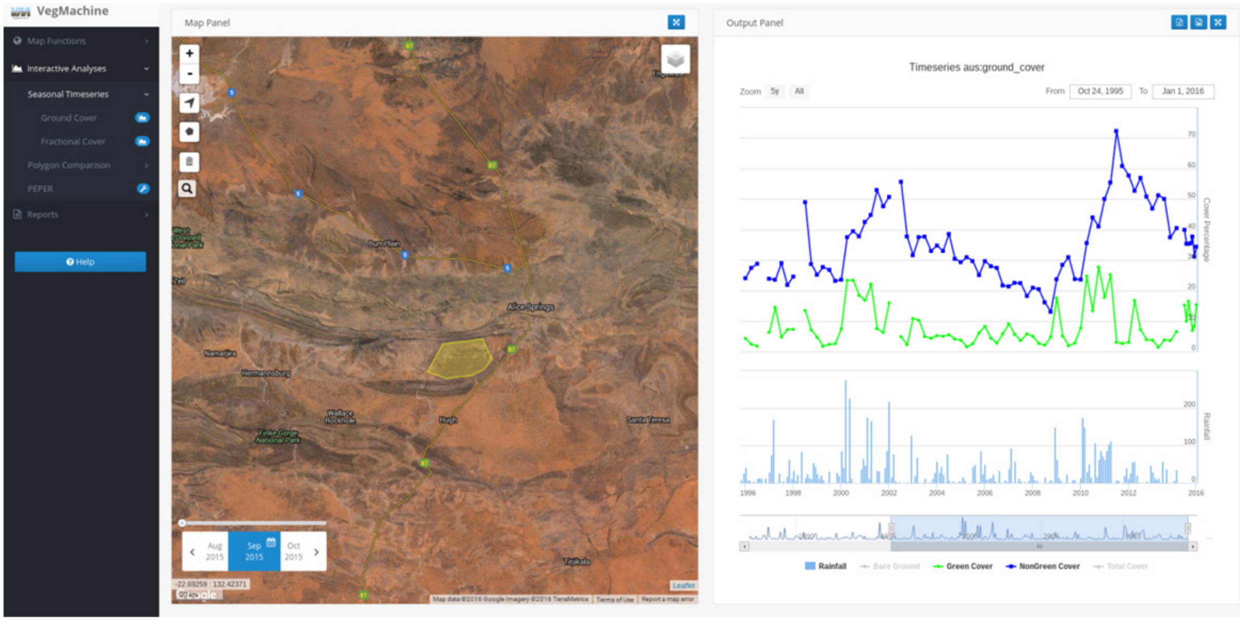

Figure 7. An example of a NPV cover time series provided through the VegMachine application developed for forage monitoring in Australia. The plot at right shows trends in NPV cover (blue line) and PV cover (green line) in context of precipitation (blue bars).

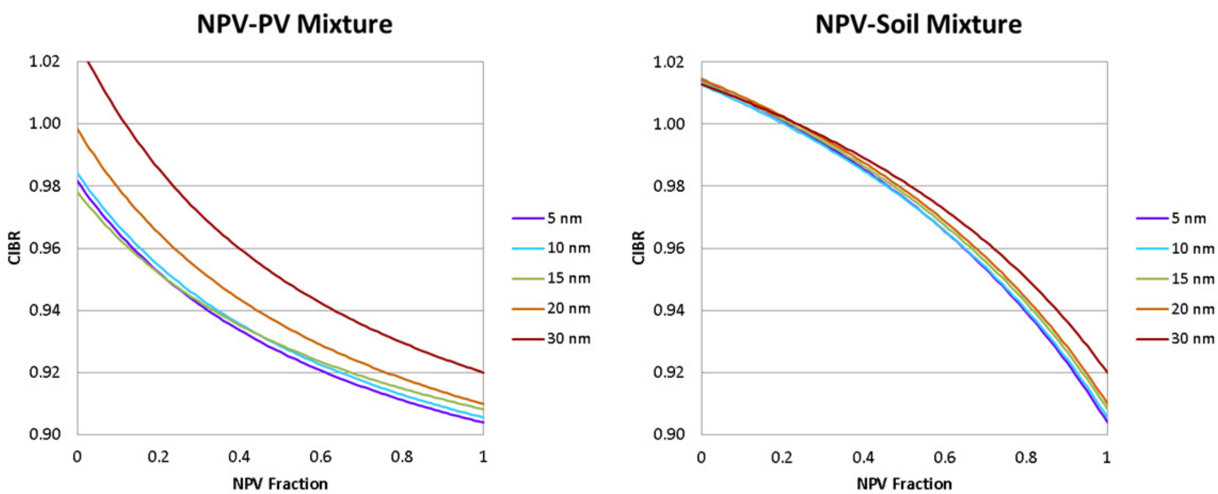

Figure 8. Continuum interpolated band ratio (CIBR) values measuring the depth of the 2120 nm lignocellulose absorption maximum across mixtures of NPV and PV spectra (left) and NPV and soil spectra (right). Lower CIBR values indicate stronger absorption and a greater ability to discriminate fractional NPV cover in mixed pixels. As spectral resolution and full-width half-maximum are degraded, there is little change in lignocellulose absorption strength through 15 nm sampling. However, the expression of lignocellulose absorption is reduced at 20 nm and 30 nm sampling.

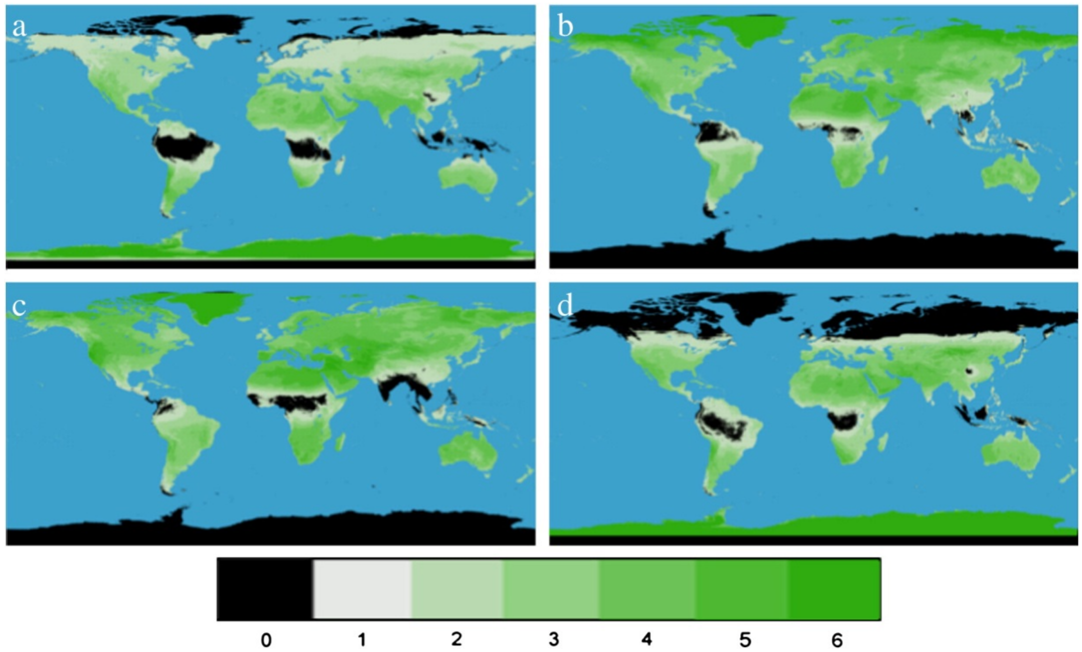

Figure 9. Number of cloud-free daytime views for a 19-day repeat cycle, for a) Jan-Mar, b) Apr-Jun, c) Jul-Sep, and d) Oct-Dec. From Mercury et al., 2012.

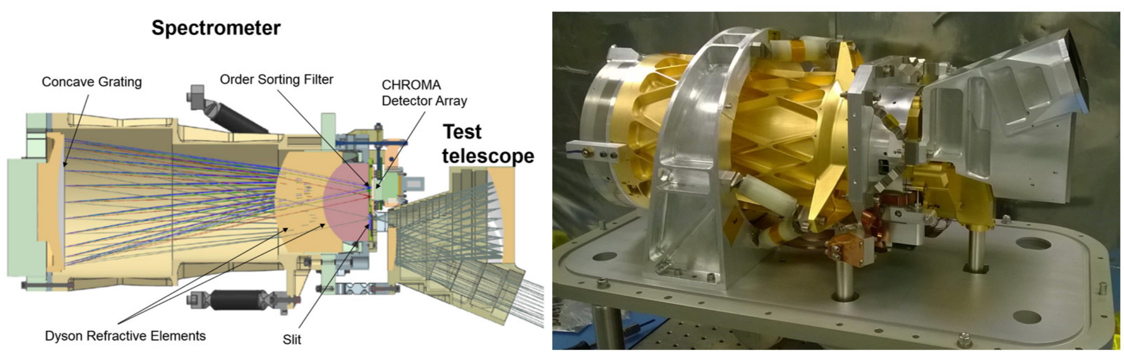

Figure 10. Design of the prototype F/1.8 VSWIR Dyson spectrometer covering a spectral range from 380 to 2510 nm.

References

Aranki, N., Bakhshi, A., Keymeulen, D., & Klimesh, M. (2009). Fast and adaptive lossless on-board hyperspectral data compression system for space applications. Paper presented at the 2009 IEEE Aerospace Conference.

Aranki, N., Keymeulen, D., Bakhshi, A., & Klimesh, M. (2009). Hardware implementation of lossless adaptive and scalable hyperspectral data compression for space. Paper presented at the Proceedings - 2009 NASA/ESA Conference on Adaptive Hardware and Systems, AHS 2009.

Asner, G. P., Borghi, C. E., & Ojeda, R. A. (2003). Desertification in central Argentina: changes in ecosystem carbon and nitrogen from imaging spectroscopy. Ecological Applications, 13(3), 629-648.

Asner, G. P., Brodrick, P. G., Anderson, C. B., Vaughn, N., Knapp, D. E., & Martin, R. E. (2016). Progressive forest canopy water loss during the 2012–2015 California drought. Proceedings of the National Academy of Sciences, 113(2), E249-E255.

Asner, G. P., & Heidebrecht, K. B. (2002). Spectral unmixing of vegetation, soil and dry carbon cover in arid regions: comparing multispectral and hyperspectral observations. International Journal of Remote Sensing, 23(19), 3939-3958.

Asner, G. P., & Heidebrecht, K. B. (2003). Imaging spectroscopy for desertification studies: comparing AVIRIS and EO-1 Hyperion in Argentina drylands. Geoscience and Remote Sensing, IEEE Transactions on, 41(6), 1283-1296.

Asner, G. P., & Heidebrecht, K. B. (2005). Desertification alters regional ecosystem–climate interactions. Global Change Biology, 11(1), 182-194.

Asner, G. P., Keller, M., Pereira Jr, R., Zweede, J. C., & Silva, J. N. (2004). Canopy damage and recovery after selective logging in Amazonia: field and satellite studies. Ecological Applications, 14(sp4), 280-298.

Brown, R. H., Baines, K. H., Bellucci, G., Bibring, J. P., Buratti, B. J., Capaccioni, F., . . . Sotin, C. (2005). The Cassini visual and infrared mapping spectrometer (VIMS) investigation. Space Science Reviews, 115(1-4), 111-168.

Bastin, G., Scarth, P., Chewings, V., Sparrow, A., Denham, R., Schmidt, M., O'Reagain, P. (2012). Separating grazing and rainfall effects at regional scale using remote sensing imagery: A dynamic reference-cover method. Remote Sensing of Environment 121, 443-457.

Beutel, T. S., Karfs, R. A., Bull, A. L., Peel, L., and Wallace, J. F. (2005). VegMachine – putting pastoralists in the picture. Agricultural Science 17, 18–20.

Beutel, T.S., Tindall, D., Denham, R., Trevithick, R., Scarth, P. Abbott, B and Holloway, C. (2014). Getting ground cover right: thresholds and baselines for a healthier reef. Report to the Reef Rescue Research and Development Program. Reef and Rainforest Research Centre Limited, Cairns (64pp.). ISBN: 978-1-925088-20-5.

Bradley, B. A., & Mustard, J. F. (2006). Characterizing the landscape dynamics of an invasive plant and risk of invasion using remote sensing. Ecological Applications, 16(3), 1132-1147.

Carlson, R. W., Weissman, P. R., Smythe, W. D., & Mahoney, J. C. (1992). Near-Infrared Mapping Spectrometer experiment on Galileo. Space Science Reviews, 60(1-4), 457-502.

CCSDS. (2015). Lossless multispectral and hyperspectral image compression, CCSDS 120.2-G-1, from http://public.ccsds.org/publications/archive/120x2g1.pdf

Chambers, J. Q., Fisher, J. I., Zeng, H., Chapman, E. L., Baker, D. B., & Hurtt, G. C. (2007). Hurricane Katrina's carbon footprint on US Gulf Coast forests. Science, 318(5853), 1107-1107.

Chambers, J.Q., Negron-Juarez, R., Marra, D.M. di Vittorio, A., Tews, J., Roberts, D., Ribeiro, G.H.P.M., Trumbore, S.E., and Higuchi, N. (2013). The steady-state mosaic of disturbance and succession across and old-growth Central Amazon forest landscape, Proceedings of the National Academy of Sciences, 110(10), 3949-3954.

Coates, A. R., Dennison, P. E., Roberts, D. A., & Roth, K. L. (2015). Monitoring the Impacts of Severe Drought on Southern California Chaparral Species using Hyperspectral and Thermal Infrared Imagery. Remote Sensing, 7(11), 14276-14291.

Daughtry, C. S. (2001). Discriminating crop residues from soil by shortwave infrared reflectance. Agronomy Journal, 93(1), 125-131.

Daughtry, C. S. T., Doraiswamy, P. C., Hunt Jr., E. R., Stern, A. J., McMurtrey III, J. E., & Prueger, J. H. (2006). Remote sensing of crop residue cover and soil tillage intensity. Soil Tillage Research 91:101-108.

Daughtry, C. S. T., Hunt Jr., E. R., Beeson, P. C., Milak, S., Lang, M. W., Serbin, G., Alfieri, J. G., McCarty, G. W., & Sadeghi, A. M. (2012). Remote sensing of soil carbon and greenhouse gas dynamics across agricultural landscapes. pp. 385-408. *In* M. A. Liebig, A. Franzluebers, R. F. Follett, (eds) Managing Agricultural Greenhouse Gases: Coordinated Agricultural Research through GRACEnet to Address our Changing Climate. Academic Press, Amsterdam.

Daughtry, C., Hunt, E., Doraiswamy, P., & McMurtrey, J. (2005). Remote sensing the spatial distribution of crop residues. Agronomy Journal, 97(3), 864-871.

Daughtry, C., Hunt, E., & McMurtrey, J. (2004). Assessing crop residue cover using shortwave infrared reflectance. Remote Sensing of Environment, 90(1), 126-134.

Davidson, E.A., Asner, G.P., Stone, T.A., Neil, C., & Figueiredo, R.O. (2008)., Objective indicators of pasture degradation from spectral mixture analysis of Landsat imagery, Journal of Geophysical Research, 113, G00B03, doi:10.1027/2007JG000622, 1-7.

Delgado, J.A. (2010). Crop residue is a key for sustaining maximum food production and for conservation of our biosphere. Journal of Soil and Water Conservation 65:111A-116A.

Elmore, A. J., Asner, G. P., & Hughes, R. F. (2005). Satellite monitoring of vegetation phenology and fire fuel conditions in Hawaiian drylands. Earth Interactions, 9(21), 1-21.

Elmore, A. J., Mustard, J. F., Manning, S. J., & Lobell, D. B. (2000). Quantifying vegetation change in semiarid environments: precision and accuracy of spectral mixture analysis and the normalized difference vegetation index. Remote Sensing of Environment, 73(1), 87-102.

Elvidge, C.D., (1990). Visible and near-infrared reflectance characteristics of dry plant materials, International Journal of Remote Sensing, 11(10), 1775-1795.

Gao, B. C., & Goetz, A. F. (1990). Column atmospheric water vapor and vegetation liquid water retrievals from airborne imaging spectrometer data. Journal of Geophysical Research: Atmospheres, 95(D4), 3549-3564.

Gao, B. C., Heidebrecht, K. B., & Goetz, A. F. H. (1993). Derivation of scaled surface reflectances from AVIRIS data. Remote Sensing of Environment, 44(2-3), 165-178.

Gao, B. C., Montes, M. J., Davis, C. O., & Goetz, A. F. H. (2009). Atmospheric correction algorithms for hyperspectral remote sensing data of land and ocean. Remote Sensing of Environment, 113(SUPPL. 1), S17-S24.

Green, R. O., Eastwood, M. L., Sarture, C. M., Chrien, T. G., Aronsson, M., Chippendale, B. J., . . . Solis, M. (1998). Imaging spectroscopy and the airborne visible/infrared imaging spectrometer (AVIRIS). Remote Sensing of Environment, 65(3), 227-248.

Green, R. O., Pieters, C., Mouroulis, P., Eastwood, M., Boardman, J., Glavich, T., . . . Wilson, D. (2011). The Moon Mineralogy Mapper (M3) imaging spectrometer for lunar science: Instrument description, calibration, on-orbit measurements, science data calibration and on-orbit validation. Journal of Geophysical Research E: Planets, 116(10).

Guerschman, J. P., Hill, M. J., Renzullo, L. J., Barrett, D. J., Marks, A. S., & Botha, E. J. (2009). Estimating fractional cover of photosynthetic vegetation, non-photosynthetic vegetation and bare soil in the Australian tropical savanna region upscaling the EO-1 Hyperion and MODIS sensors. Remote Sensing of Environment, 113(5), 928-945.

Guerschman, J. P., Scarth, P. F., McVicar, T. R., Renzullo, L. J., Malthus, T. J., Stewart, J. B., Rickards, J. E., Trevithick, R. (2015). Assessing the effects of site heterogeneity and soil properties when unmixing photosynthetic vegetation, non-photosynthetic vegetation and bare soil fractions from Landsat and MODIS data. Remote Sensing of Environment, 161, 12-26.

Hamlin, L., Green, R., Mouroulis, P., Eastwood, M., Wilson, D., Dudik, M., & Paine, C. (2011). Imaging spectrometer science measurements for terrestrial ecology: AVIRIS and new developments. Paper presented at the Aerospace Conference, 2011 IEEE.

Hampton, D. L., Baer, J. W., Huisjen, M. A., Varner, C. C., Delamere, A., Wellnitz, D. D., . . . Klaasen, K. P. (2005). An overview of the instrument suite for the Deep Impact mission.. Space Science Reviews, 117(1-2), 43-93.

Herrick, J. E., Van Zee, J. W., Havstad, K. M., Burkett, L. M., & Whitford, W. G. (2005). Monitoring manual for grassland, shrubland and savanna ecosystems. Volume I: Quick Start. Volume II: Design, supplementary methods and interpretation. Las Cruces, New Mexico: USDA-ARS Jornada Experimental Range.

Jia, G. J., Burke, I. C., Goetz, A. F., Kaufmann, M. R., & Kindel, B. C. (2006). Assessing spatial patterns of forest fuel using AVIRIS data. Remote Sensing of Environment, 102(3), 318-327.

Karfs R. A., Abbott B. N., Scarth P. F., Wallace J. F. (2009). Land condition monitoring information for reef catchments: a new era. The Rangeland Journal 31, 69-86.

Karlen, D., Wollenhaupt, N. C., Erbach, D., Berry, E., Swan, J., Eash, N., & Jordahl, J. (1994). Crop residue effects on soil quality following 10-years of no-till corn. Soil and Tillage Research, 31(2), 149-167.

Keymeulen, D., Aranki, N., Bakhshi, A., Luong, H., Sarture, C., & Dolman, D. (2014). Airborne demonstration of FPGA implementation of Fast Lossless hyperspectral data compression system. Paper presented at the Proceedings of the 2014 NASA/ESA Conference on Adaptive Hardware and Systems, AHS 2014.

Klimesh, M. (2006). Low-complexity adaptive lossless compression of hyperspectral imagery. Paper presented at the Proceedings of SPIE - The International Society for Optical Engineering.

Kokaly, R. F., Asner, G. P., Ollinger, S. V., Martin, M. E., & Wessman, C. A. (2009). Characterizing canopy biochemistry from imaging spectroscopy and its application to ecosystem studies. Remote Sensing of Environment, 113, S78-S91.

Kokaly, R. F., & Clark, R. N. (1999). Spectroscopic determination of leaf biochemistry using band-depth analysis of absorption features and stepwise multiple linear regression. Remote Sensing of Environment, 67(3), 267-287.

Kokaly, R.F., King, T.V.V., and Hoefen, T.M. (2013). Surface mineral maps of Afghanistan derived from HyMap imaging spectrometer data, version 2: U.S. Geological Survey Data Series 787, 29p., http://pubs.usgs.gov/ds/787/.

Kokaly, R. F., Rockwell, B. W., Haire, S. L., & King, T. V. (2007). Characterization of post-fire surface cover, soils, and burn severity at the Cerro Grande Fire, New Mexico, using hyperspectral and multispectral remote sensing. Remote Sensing of Environment, 106(3), 305-325.

Lal, R., Reicosky, D., & Hanson, J. (2007). Evolution of the plow over 10,000 years and the rationale for no-till farming. Soil and Tillage Research, 93(1), 1-12.

Lee, C. M., Cable, M. L., Hook, S. J., Green, R. O., Ustin, S. L., Mandl, D. J., & Middleton, E. M. (2015). An introduction to the NASA Hyperspectral InfraRed Imager (HyspIRI) mission and preparatory activities. Remote Sensing of Environment, 167, 6-19.

Lewis, S. A., Hudak, A. T., Ottmar, R. D., Robichaud, P. R., Lentile, L. B., Hood, S. M., . . . Morgan, P. (2011). Using hyperspectral imagery to estimate forest floor consumption from wildfire in boreal forests of Alaska, USA. International journal of wildland fire, 20(2), 255-271.

Lewis, S. A., Lentile, L. B., Hudak, A. T., Robichaud, P. R., Morgan, P., & Bobbitt, M. J. (2007). Mapping ground cover using hyperspectral remote sensing after the 2003 Simi and Old wildfires in Southern California.

Littell, J. S., McKenzie, D., Peterson, D. L., & Westerling, A. L. (2009). Climate and wildfire area burned in western US ecoprovinces, 1916-2003. Ecological Applications, 19(4), 1003-1021.

McGregor, K., & Greer, J. (1982). Erosion control with no-till and reduced till corn for silage and grain. Transactions of the ASAE, 25(1), 154-0159.

Mercury, M., Green, R., Hook, S., Oaida, B., Wu, W., Gunderson, A., & Chodas, M. (2012). Global cloud cover for assessment of optical satellite observation opportunities: A HyspIRI case study. Remote Sensing of Environment, 126, 62-71.

Meyer, T., & Okin, G. (2015). Evaluation of spectral unmixing techniques using MODIS in a structurally complex savanna environment for retrieval of green vegetation, nonphotosynthetic vegetation, and soil fractional cover. Remote Sensing of Environment, 161, 122-130.

Mouroulis, P., Green, R. O., Van Gorp, B., Moore, L. B., Wilson, D. W., & Bender, H. A. (2016). Landsat swath imaging spectrometer design. Optical Engineering, 55(1).

Murchie, S., Arvidson, R., Bedini, P., Beisser, K., Bibring, J. P., Bishop, J., . . . Wolff, M. (2007). Compact Connaissance Imaging Spectrometer for Mars (CRISM) on Mars Reconnaissance Orbiter (MRO). Journal of Geophysical Research E: Planets, 112(5).

Nagler, P., Daughtry, C., & Goward, S. (2000). Plant litter and soil reflectance. Remote Sensing of Environment, 71(2), 207-215.

Nagler, P. L., Inoue, Y., Glenn, E., Russ, A., & Daughtry, C. (2003). Cellulose absorption index (CAI) to quantify mixed soil–plant litter scenes. Remote Sensing of Environment, 87(2), 310-325.

NRC. (2007). Earth Science and Applications from Space: National Imperatives for the Next Decade and Beyond. Washington, DC: The National Academies Press.

NRC. (2013). Landsat and Beyond: Sustaining and Enhancing the Nation's Land Imaging Program. Washington, DC: The National Academies Press.

Negrón-Juárez, R. I., Chambers, J. Q., Marra, D. M., Ribeiro, G. H., Rifai, S. W., Higuchi, N., & Roberts, D. (2011). Detection of subpixel treefall gaps with Landsat imagery in Central Amazon forests. Remote Sensing of Environment, 115(12), 3322-3328.

Numata, I., Roberts, D. A., Chadwick, O. A., Schimel, J., Sampaio, F. R., Leonidas, F. C., & Soares, J. V. (2007). Characterization of pasture biophysical properties and the impact of grazing intensity using remotely sensed data. Remote Sensing of Environment, 109(3), 314-327.

Numata, I., Roberts, D. A., Chadwick, O. A., Schimel, J. P., Galvão, L. S., & Soares, J. V. (2008). Evaluation of hyperspectral data for pasture estimate in the Brazilian Amazon using field and imaging spectrometers. Remote Sensing of Environment, 112(4), 1569-1583.

Okin, G. S. (2007). Relative spectral mixture analysis—A multitemporal index of total vegetation cover. Remote Sensing of Environment, 106(4), 467-479.

Okin, G.S. (2010). The contribution of brown vegetation to vegetation dynamics. Ecology. 91(3), 743-755.

Okin, G. S., & Gu, J. (2015). The impact of atmospheric conditions and instrument noise on atmospheric correction and spectral mixture analysis of multispectral imagery. Remote Sensing of Environment, 164, 130-141.

Okin, G. S., & Roberts, D. A. (2004). Remote sensing in arid regions: challenges and opportunities. In S. L. Ustin (Ed.), Manual of Remote Sensing: Remote sensing for natural resource management and environmental monitoring (pp. 111-146). New York: John Wiley and Sons.

Okin, G. S., Roberts, D. A., Murray, B., & Okin, W. J. (2001). Practical limits on hyperspectral vegetation discrimination in arid and semiarid environments. Remote Sensing of Environment, 77(2), 212-225.

Pasto, J. K., Allison, J. R., & Washko, J. B. (1957). Ground cover and height of sward as a means of estimating pasture production. Agronomy Journal, 49(8), 407-409.

Pearlman, J. S., Barry, P. S., Segal, C. C., Shepanski, J., Beiso, D., & Carman, S. L. (2003). Hyperion, a space-based imaging spectrometer. IEEE Transactions on Geoscience and Remote Sensing, 41(6 PART I), 1160-1173.

Qi, Y., Dennison, P. E., Jolly, W. M., Kropp, R. C., & Brewer, S. C. (2014). Spectroscopic analysis of seasonal changes in live fuel moisture content and leaf dry mass. Remote Sensing of Environment, 150, 198-206.

Roberts, D., Dennison, P., Peterson, S., Sweeney, S., & Rechel, J. (2006). Evaluation of Airborne Visible/Infrared Imaging Spectrometer (AVIRIS) and Moderate Resolution Imaging Spectrometer (MODIS) measures of live fuel moisture and fuel condition in a shrubland ecosystem in southern California. Journal of Geophysical Research: Biogeosciences, 111(G4).

Roberts, D., Green, R., & Adams, J. (1997). Temporal and spatial patterns in vegetation and atmospheric properties from AVIRIS. Remote Sensing of Environment, 62(3), 223-240.

Roberts, D., Smith, M., & Adams, J. (1993). Green vegetation, nonphotosynthetic vegetation, and soils in AVIRIS data. Remote Sensing of Environment, 44(2), 255-269.

Scarth, P., & Phinn, S. (2000). Determining forest structural attributes using an inverted geometric-optical model in mixed eucalypt forests, Southeast Queensland, Australia. Remote Sensing of Environment, 71(2), 141-157.

Scarth, P., Röder, A., Schmidt, M., & Denham, R. (2010). Tracking grazing pressure and climate interaction—The role of Landsat fractional cover in time series analysis. Paper presented at the Proceedings of the 15th Australasian Remote Sensing and Photogrammetry Conference, Alice Springs, Australia.

Serbin, G., Daughtry, C. S., Hunt, E. R., Brown, D. J., & McCarty, G. W. (2009b). Effect of soil spectral properties on remote sensing of crop residue cover. Soil Science Society of America Journal, 73(5), 1545-1558.

Serbin, G., Hunt Jr, E. R., Daughtry, C. S., & McCarty, G. W. (2013). Assessment of spectral indices for cover estimation of senescent vegetation. Remote Sensing Letters, 4(6), 552-560.

Serbin, G., Hunt, E. R., Daughtry, C. S., McCarty, G. W., & Doraiswamy, P. C. (2009a). An improved ASTER index for remote sensing of crop residue. Remote Sensing, 1(4), 971-991.

Serbin, S. P., Singh, A., McNeil, B. E., Kingdon, C. C., & Townsend, P. A. (2014). Spectroscopic determination of leaf morphological and biochemical traits for northern temperate and boreal tree species. Ecological Applications, 24(7), 1651-1669.

Singh, A., Serbin, S. P., McNeil, B. E., Kingdon, C. C., & Townsend, P. A. (2015). Imaging spectroscopy algorithms for mapping canopy foliar chemical and morphological traits and their uncertainties. Ecological Applications, 25(8), 2180-2197.

Star, M., Rolfe, J., Donaghy, P., Beutel, T., Whish, G., & Abbott, B. (2013). Targeting resource investments to achieve sediment reduction and improved Great Barrier Reef health. *Agriculture, ecosystems & environment*, *180*, 148-156.

Thompson, D. R., Gao, B.-C., Green, R. O., Roberts, D. A., Dennison, P. E., & Lundeen, S. R. (2015). Atmospheric correction for global mapping spectroscopy: ATREM advances for the HyspIRI preparatory campaign. Remote Sensing of Environment, 167, 64-77.

Thompson, D. R., Green, R. O., Keymeulen, D., Lundeen, S. K., Mouradi, Y., Nunes, D. C., . . . Chien, S. A. (2014). Rapid spectral cloud screening onboard aircraft and spacecraft. IEEE Transactions on Geoscience and Remote Sensing, 52(11), 6779-6792.

Van Gorp, B., Mouroulis, P., Wilson, D. W., & Green, R. O. (2014). Design of the compact wide swath imaging spectrometer (CWIS). Paper presented at the Proceedings of SPIE - The International Society for Optical Engineering.

Van Leeuwen, W., & Huete, A. (1996). Effects of standing litter on the biophysical interpretation of plant canopies with spectral indices. Remote Sensing of Environment, 55(2), 123-138.

Van Wagtendonk, J. W., Root, R. R., & Key, C. H. (2004). Comparison of AVIRIS and Landsat ETM+ detection capabilities for burn severity. Remote Sensing of Environment, 92(3), 397-408.

Vane, G., Goetz, A. F., & Wellman, J. B. (1984). Airborne imaging spectrometer: A new tool for remote sensing. Geoscience and Remote Sensing, IEEE Transactions on (6), 546-549.

Veraverbeke, S., & Hook, S. J. (2013). Evaluating spectral indices and spectral mixture analysis for assessing fire severity, combustion completeness and carbon emissions. International journal of wildland fire, 22(5), 707-720.

Veraverbeke, S., Stavros, E. N., & Hook, S. J. (2014). Assessing fire severity using imaging spectroscopy data from the Airborne Visible/Infrared Imaging Spectrometer (AVIRIS) and comparison with multispectral capabilities. Remote Sensing of Environment, 154, 153-163.

Zheng, B., Campbell, J., Serbin, G., & Daughtry, C. (2013). Multitemporal remote sensing of crop residue cover and tillage practices: A validation of the minNDTI strategy in the United States. Journal of Soil and Water Conservation, 68(2), 120-131.